Synthesis and Relaxation Dynamics of Multiarm Polybutadiene Melts

L. A. Archer*

Department of Chemical Engineering, Texas A&M University, College Station, Texas 77843

S. K. Varshney

Polymer Source Inc., Dorval, PQ, Canada H9P 1G7

Received February 20, 1998; Revised Manuscript Received May 26, 1998

ABSTRACT: We describe synthesis and nonlinear relaxation dynamics of various multiarm entangled polybutadiene molecules of the general type A_3-**A**-A_3. In low-amplitude oscillatory shear, entangled multiarm polymers display broader relaxation spectra than linear polybutadienes of comparable molecular weight. Dramatic slowing down of cross-bar (**A**) relaxation by the entangled arms (*A*) is believed to be the source of this behavior. In nonlinear step strain experiments the *A* arms have a rather remarkable effect on polymer dynamics. At a critical shear strain γ of around 6.0, $\langle|E\cdot u|\rangle = 3.2$, the nonlinear relaxation modulus $G(t;\gamma)$ abruptly decreases in value but retains similar time dependence to $G(t;\gamma)$ at strains below the critical value. The sudden drop in $G(t;\gamma)$ is reflected in the damping function and appears to be a consequence of arm withdrawal into the tube confining the cross-bar. This behavior is in near perfect agreement with a recent theoretical proposal for branched polymer dynamics. That this proposal is based on the notion of tensile forces on individual macromolecules due to tube confinement supports the existence of such forces and provides new circumstantial evidence for the existence of a mean-field tube. For all multiarm polymers studied we find time−strain separability at all strains with a separability time λ_k that appears insensitive to the arm withdrawal process. This last finding is not in agreement with current descriptions of multiarm polymer dynamics.

1.0. Introduction

Linear viscoelastic properties and relaxation dynamics of branched macromolecules has attracted considerable research interest in the last several years. This interest is sustained by the commercial importance of branched polymers and by the challenge of generalizing to other architectures theoretical constructs such as the tube that appears to capture linear polymer dynamics. Detailed rheology studies have emerged for architectures including multiarm stars,[1−4] comb polymers,[5,6] and H-shaped molecules.[7−9] In all cases material properties such as zero shear viscosity and terminal molecular relaxation time manifest exponential dependences on arm molecular weight. When arm molecular weights are large enough to form entanglements, orders of magnitude enhancements in zero shear viscosity and stress relaxation times are found relative to linear polymers of comparable molecular weight.

McLeish[9] and recently Bick and McLeish[10] and Bishko et al.[11] proposed a molecular theory for multiarm polymer dynamics that provides a promising starting point for describing the nonlinear rheology of entangled branched polymers. The theory is based on the tube model picture, which assumes that neighboring polymer molecules entangle with each other and thereby impose topological constraints that restrict motion of individual macromolecules to a tubelike region of diameter $a = \sqrt{N_e}b$ that follows the molecular contour. N_e is the number of chain segments between entanglement points, and b is the segment length. The main innovation in the theory of McLeish et al.[9−11] concerns the way arm friction is introduced into the nonlinear relaxation modulus. Specifically, for a multiarm polymer molecule as in Figure 1 these authors contend that the nonlinear relaxation modulus should change dramatically when the effective tube strain $\langle|E\cdot u|\rangle$ approaches the *priority*

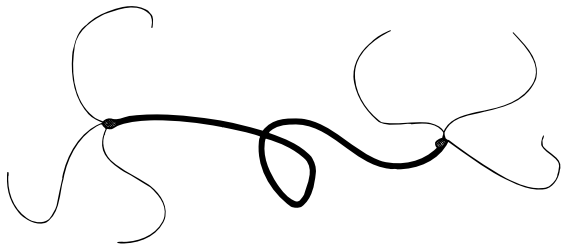

Figure 1. Molecular architecture of A_3-**A**-A_3 multiarm polybutadiene. The central portion of the molecule (cross-bar) is 55% 1,4-polybutadiene and the arms are >92% 1,4-polybutadiene.

i (minimum number of arms) of the molecule. At strains such that $\langle|E\cdot u|\rangle < i$ retraction of the central portion of the molecule (cross-bar) is thought to be prevented by a Pincus law tensile force that pulls the outermost segments of the arms away from the branch point. For fully relaxed arms this force is $F_{eq} = 3k_BT/a$ per arm, which is large enough to overcome the affine tension in the cross bar $F = 3(k_BT/a)\langle|E\cdot u|\rangle$.[12] As a result, the contour length of the cross-bar retains it instantaneous affine value $L = L_o\langle|E\cdot u|\rangle$ even after the arms have relaxed completely. This situation changes when the tube strain exceeds the priority of the molecule, $\langle|E\cdot u|\rangle \geq i$. In this case the affine tension in the cross-bar becomes large enough to overcome the total outward force $F_{eq;T} = 3i(k_BT/a)$ on the arms, allowing the arms to be withdrawn into the central tube.

Assuming time strain facotorability occurs after some period of time, the effect of strain on the nonlinear modulus can be separated into two parts, $h_{el}(\gamma) = [\langle|E\cdot u|\rangle/(4/15)\gamma]\langle(E\cdot u)(E\cdot u)/|E\cdot u|\rangle$ and $h_{DE}(\gamma) = [1/(4/15)\gamma - \langle|E\cdot u|\rangle]\langle(E\cdot u)(E\cdot u)/|E\cdot u|\rangle$ for $\langle|E\cdot u|\rangle < i$ and $\langle|E\cdot u|\rangle > i$, respectively.[10] The predicted discontinuity in the shear damping function is smoothed out in real branched polymers by an inevitable distribution of priorities. For

S0024-9297(98)00273-3 CCC: $15.00
Published on Web 08/19/1998

well-defined multiarm polymers where all molecules have the same priority, the discontinuity should persist and could be compared with experimental results to evaluate the new proposal.

In addition to the abrupt change in shear damping function at the critical tube strain $\langle|E\cdot u|\rangle = i$, a dramatic change in the time dependence of the nonlinear modulus is anticipated. This last effect has recently been described by Bishko et al.[11] and by McLeish and Larson.[13] These authors show that at strains below the critical value the transient nonlinear relaxation modulus of a branched polymer with moderately entangled arms is qualitatively identical to that of a linear one. The only differences being that all characteristic time scales are modulated by the arm disengagement time instead of by the longest Rouse time of the polymer. The stretch relaxation time λ_s (the time required for a polymer's contour length to return to its equilibrium value) is for instance no longer related to the longest Rouse time for the primitive chain, but rather to the arm disengagement time λ_a, $\lambda_s \approx is_b\lambda_a$. Likewise, the polymer disengagement time λ_d is no longer the reptation time λ of the primitive chain, but rather $\lambda_d \approx is_b^2\phi_b\lambda_a$. Here $\phi_b \equiv s_b/(s_b + 2is_a)$ is the fraction of cross-bar segments that, to the arms, appear dynamically frozen; $s_b = N_b/N_e$ is the cross-bar entanglement density and $s_a = N_a/N_e$ is the arm entanglement density. The situation changes when the strain exceeds the critical value because arms can now be withdrawn by the affine cross-bar tension into the central tube. As a result, the arm relaxation time itself becomes time-dependent and stretch relaxation becomes dynamically coupled to the details of the arm withdrawal process. Any dynamic similarity to linear polymers obviously disappears at this point.

In this paper we describe the synthesis of model entangled multiarm polybutadiene melts of the type shown in Figure 1 and use them to evaluate several of the ideas outlined in the previous section. Unlike commercial polymers where cross-bar contour length and priority may vary considerably from molecule to molecule, thereby reducing the abruptness of the transition anticipated from the theory, the studied materials are synthesized with narrow molecular weight distributions and well-defined number of branches. Polybutadiene was chosen for three reasons: (i) The material forms a room temperature melt, which facilitates measurements at ambient temperature. (ii) The entanglement molecular weight of the material, $M_e \approx 2100$,[14] is low enough that polymers of the desired architecture can be synthesized with well entangled arms and crossbars. (iii) Relaxation times for linear polybutadiene melts are accessible even for extremely high entanglement densities (for example, the terminal time of a linear polybutadiene melt with $N/N_e = 308$ is just 28 s) at room temperature, which should guarantee multiarm polymer relaxation time scales that are not so excessive as to negate benefit (i).

2.0. Experimental Section

2.1. Polymer Synthesis. Chemicals. Butadiene (Matheson Co.) was condensed after passing through a column containing freshly crushed CaH_2 and then distilled over *n*-BuLi just prior to use. Styrene (Aldrich Chemical Co.) was dried over CaH_2 for 2 days, then kept over fluorenyllithium, and distilled just before use. 1,3-Diisopropenylbenzene (DIB), diphenylethylene, and triethylamine (Et_3N from Aldrich Chemical Co.) were dried over CaH_2 for 1 day, distilled over fluorenyllithium, and then diluted with dry benzene. Silicon tetrachloride (99.99% obtained from Aldrich) was dried over CaH_2 for 1 day and distilled. Commercially available *t*-BuLi was analyzed by a double titration method with 1,2-dibromobutane. Benzene and diethyl ether were refluxed over CaH_2 for several days. All solvents were further dried by adding with living polystyryllithium oligmers and distilled just prior to use.

Preparation of *t*-BuLi/1,3-DIB Diinitiator. Difunctional initiator obtained by addition reaction of a mixture of *t*-BuLi/Et_3N (1:1 molar ratio) to 1,3-diisopropenylbenzene in a 2:1 molar ratio was prepared in benzene according to the method reported by Jerome et al.[15] Difunctional initiator was obtained in benzene at a concentration of 10^{-3} mol·L^{-1}. The optimized reaction conditions include dropwise addition of 1,3-diisopropenylbenzene in benzene to a stirred benzene solution of a 1:1 *t*-BuLi−Et_3N complex at −10 °C. A dark green color was immediately developed after the addition of *t*-BuLi-Et_3N mixture onto 1,3-diisopropenylbenzene. The solution was stirred for 10 min at −10 °C followed by a 30 min postreaction period at ice bath temperatures. The dark green color of the solution changes to a deep dark homogeneous red color solution.

Polymerization Procedure. The synthesis of multiarm architecture A_3-**A**-A_3 was performed in two steps.

(1) Synthesis of α,ω-bis(trichlorosilyl)polybutadiene central block: The polymerization was carried out under vacuum in a specially constructed 250 mL round bottom flask connected with three side arms glass break-seals. Syringes and stainless steel capillaries were used in order to transfer solvent, monomer, and initiator. Polymerization was carried out in benzene containing 10% by volume diethyl ether. A known quantity of difunctional initiator was charged followed by addition of a 2 molar excess of styrene (with respect to the initiator). A deep orange red color developed. The solution was stirred for 5 min at ice bath temperature. Butadiene was slowly added to the initiator solution. The deep red-orange color discharged to a light yellow color. The reactor was sealed off under vacuum. The solution was stirred for 1 day at room temperature. A 3 times molar excess of purified diphenylethylene (with respect to the initiator) was added to end-cap the living dilithiopolybutadiene macroanions. The solution was stirred at room temperature for 4 h, and a deep orange red color developed. The solution was transferred to a large excess of vigorously stirred, purified silicon tetrachloride (2000 molar excess with respect to the initiator). All these manipulations were carried out in a closed system under vacuum utilizing a break-seal technique. The deactivation of α,ω-dilithio macroanions of polybutadiene with $SiCl_4$ was carried out at the ice bath temperature. A small quantity of polymer was transferred to the side arm of the flask, for molecular weight determination of the center block by size exclusion chromatography. The obtained α,ω-bis(trichlorosilyl)polybutadiene block was purified by removing the excess of $SiCl_4$ under vacuum followed by freeze drying in purified dry benzene.

(2) Synthesis of polybutadiene side arm -*A* and linkage: Polybutadiene was prepared in a specially constructed 250 mL round bottom flask connected through the side arm by a break-seal to another 250 mL flask containing purified α,ω-bis-(trichlorosilyl)polybutadiene. Polymerization of purified butadiene monomer was initiated by *s*-BuLi in benzene at room temperature overnight. The obtained living polybutadieneyllithium was added (10 times molar excess with respect to α,ω-bis(trichlorosilyl)polybutadiene) to α,ω-bis(trichlorosilyl)polybutadiene through the side arm. The linking reaction was performed at 35 °C for 1 day. The color of the solution changed from light yellow to a deep red color in about 7−8 h of reaction time. The color change indicates the completion of the linking reaction. The appearance of the red color is due to the presence of excess diphenylethylene used in end capping dilithiopolybutadiene macroanions for the synthesis of the α,ω-bis(trichlorosilyl)polybutadiene central block. The final A_3-**A**-A_3 multiarm product was separated from the unlinked polybutadiene homopolymer by repeated fractionation in toluene/methanol at a 30 °C bath temperature.

Scheme 1. Schematic Methodology Used To Synthesize A_3-A-A_3 Multiarm Polybutadiene Polymers (Sample P1132)

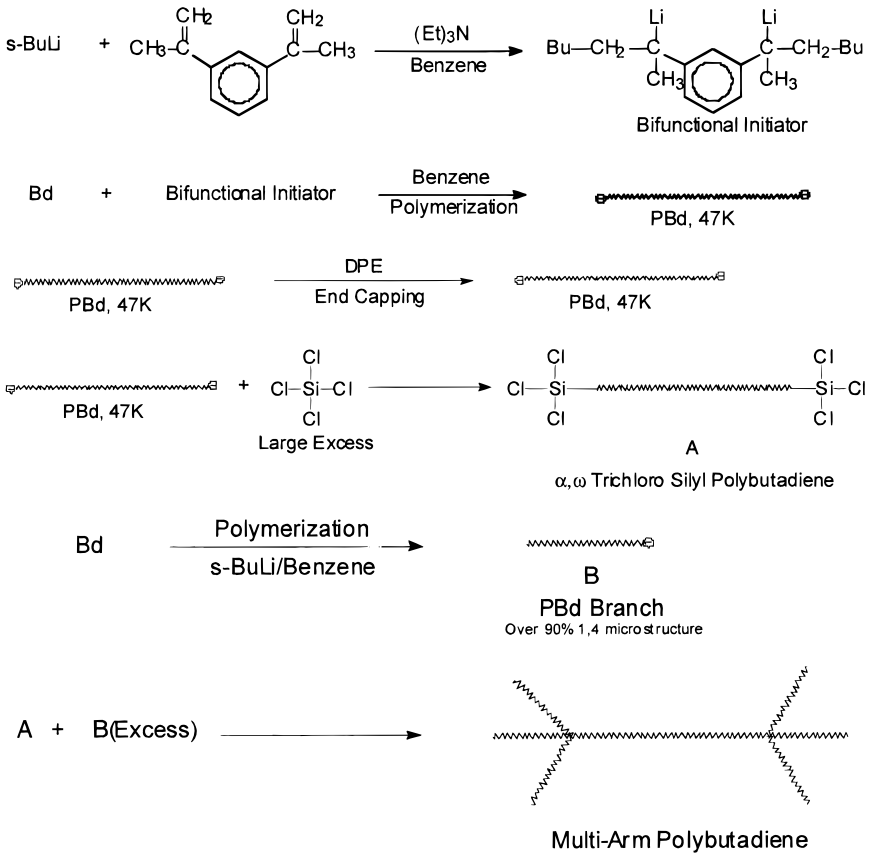

Table 1. Molecular Parameters for Linear and Multiarm A_3-A-A_3 Polybutadienes

sample	$\bar{M}_n$ of Center **A** block[a]	$10^{-4}\bar{M}_n$ of *A* arms[b]	$\bar{M}_w/\bar{M}_n$ of polymer[c]
PBD86	8.65×10^4		1.04
PBD129	1.29×10^5		1.03
PBD176	1.76×10^5		1.03
P1134	4.70×10^4	1.48	1.15
P1184	3.52×10^4	1.40	1.15
P1132	4.70×10^4	1.95	1.15
P1210	9.07×10^4	1.20	1.08
P1207	9.07×10^4	1.95	1.11

[a] HNMR analysis indicates 55% 1-4 addition. [b] HNMR analysis indicates 92% 1-4 addition. [c] Multiarm polymer molecular weights measured relative to linear polybutadiene standards.

Characterization. The molecular weights, molecular weight distributions, and purity of the final A_3-**A**-A_3 multiarm polymers and the intermediate products were evaluated by size exclusion chromatography (SEC) in THF at 30 °C (Varian 9002 pump, 9300 auto sample injector, RI-4 differential refractometer, 9050 variable-wavelength UV detector in series with three Supelco G6000, 4000, 2000 HXL linear columns). The SEC instrument was calibrated with monodisperse polybutadiene standards. ^{1}H NMR spectroscopy was carried out on a 400 MHz Bruker spectrophotometer in $CDCl_3$ at room temperature.

Results. The new multiarm architecture A_3-**A**-A_3 based on polybutadiene as shown schematically in Figure 1 was synthesized by anionic living polymerization. Various multiarm polymers were synthesized with different degrees of polymerization for both the central A block of polybutadiene and terminal arm A blocks. The synthesis route for this multiarm architecture A_3-**A**-A_3 is illustrated in Scheme 1 and is similar to those reported by Roovers and Toporowski and by Hakki et al. for the synthesis of H-shaped polymers.[7,16] Table 1 describes the molecular characteristics of various multiarm architecture polymers.

Difunctional initiator used for the synthesis of the center A block was based on an adduct of a 2 molar excess of *t*-BuLi with respect to 1,3-diisopropenylbenzene in the presence of Et_3N. In all cases close agreement between the calculated stoichiometric molecular weights, assuming perfect difunctionality, and the experimentally determined molecular weights was observed. The molecular weight distributions of the resulting α,ω-bis(trichlorosilyl)polybutadiene obtained after deactivation of α,ω-dilithiopolybutadiene macroanions with a large excess of $SiCl_4$, determined by SEC, were always monomodal. The corresponding SEC chromatograms for one of the batch P1132 are shown in Figure 2. The ^{1}H NMR analysis of the center block indicates 55% 1,4 addition due to the presence of 10 vol % diethyl ether. The ^{1}H NMR spectrum of the side arms polybutadiene indicated over 92% 1,4 addition of butadiene.

2.2. Rheological Characterization. Linear viscoelastic properties of the multiarm polymers were characterized by oscillatory shear rheometry and small amplitude step strain measurements. Measurements were performed at 24.5 °C using a Paar Physica Universal Dynamic spectrometer (UDS) equipped with cone and plate stainless steel fixtures. Cones of 25 and 15 mm diameter, (cone angle 1°) were used for the oscillatory shear measurements whereas 15 mm diameter (cone angle 1°) and 8 mm diameter (cone angle 2°) cones were used for the step strain measurements. Higher instantaneous torques generated on imposition of step strains, particularly in the nonlinear viscoelastic regime (see section 3.0), precluded safe use of the larger diameter cones in the nonlinear step strain experiments. Nonlinear step strain experiments were cross-checked using the 15 and 8 mm diameter cones. Except at short times (within the first second following imposition of nonlinear step strain), axial compliance errors were found to be negligible for all materials investigated in this study.

In the oscillatory shear experiments, strain amplitudes were maintained below 4% at shear frequencies above the $G' - G''$ crossover frequency and below 16% for frequencies below the crossover value. In this way the deformation was maintained

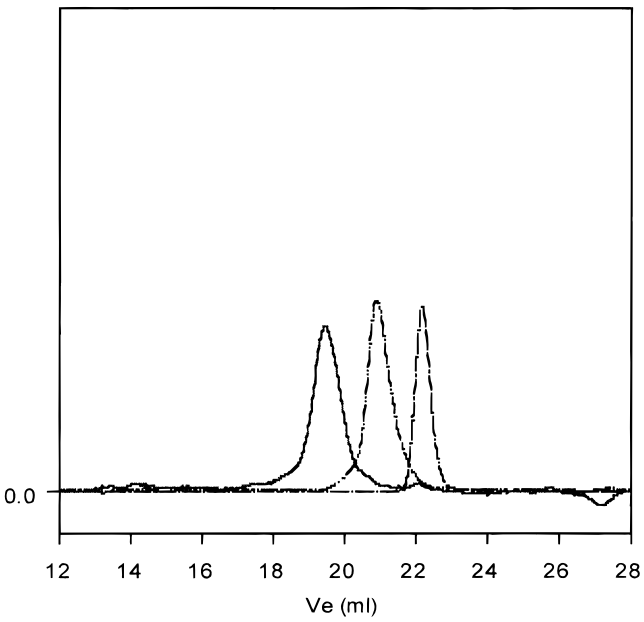

Figure 2. Size exclusion chromatography (SEC) profile of sample P1132: (− −) PBd branch, $M_n = 19\,500$, $M_w = 20\,085$, $M_w/M_n = 1.03$; (−·−) α,ω-bis(trichlorosilyl)PBd backbone, $M_n = 47\,000$, $M_w = 51\,700$, $M_w/M_n = 1.10$; (—) final multiarm PBd with respect to linear PBd standards, $M_n = 154\,300$, $M_w/M_n = 1.15$.

in the linear regime for all samples. A constant strain amplitude of 20% was used for the linear step strain measurements.

Zero shear viscosities $\eta_0 = \lim_{\omega\to 0} [G''(\omega)/\omega]$, $G' - G''$ crossover frequencies ω_c, and plateau moduli G_N of all polymer samples used in the study were deduced from the oscillatory shear measurements. The plateau modulus for the multiarm materials was estimated as their storage modulus value at the frequency where the loss tangent $\tan\delta = G''(\omega)/G'(\omega)$ displays a local minimum. For the linear polymers the loss tangent minimum is not seen in the range of frequencies and temperatures of the study. In this case, the plateau modulus was estimated from the steady-state recoverable creep compliance $G_N \approx 2.4/J_e^\circ$, where

$$J_e^\circ = (1/\eta_0^2) \lim_{\omega\to 0} \left[\frac{G'(\omega)}{\omega^2}\right]$$

Tube disengagement times λ_d for all materials studied were determined from the long-time (times exceeding the separability time, λ_k) slope of $\log_e \sigma$ versus time plots following linear step strain.

3.0. Results and Discussion

Storage and loss moduli for samples P1184, P1132, and P1134 are presented in Figure 3a,b, respectively. To facilitate comparison with typical linear polymer behavior, the figures also include data from a linear polybutadiene melt (PBD129) with a number average molecular weight $\bar{M}_n = 1.29 \times 10^5$, which is close to the overall molecular weights of the multiarm polymers. Similar results for P1207 and P1210 are presented in Figure 3c,d, where the comparison is with data from two linear polymers, PBD86 $\bar{M}_n = 8.65 \times 10^4$ and PBD176 $\bar{M}_n = 1.76 \times 10^5$, with molar masses close to the cross-bar molecular weight and the overall multiarm polymer molecular weight, respectively. Quantitative rheological information deduced from the plots is presented in Table 2.

Parts a−d of Figure 3 reveal at least three features of multiarm entangled polymer behavior that appear unique. First, the relaxation spectra of these materials are significantly broader than those of the linear polymers. In the series PBD86−P1207, for instance, the transition to terminal behavior is seen to be shifted downward in frequency by some 4 orders of magnitude even though the maximum arm entanglement density is only 9. The qualitative effect of the arms on overall polymer relaxation can be seen by comparing ω_c values of P1132 and P1134; these two materials have identical cross-bar molecular weights and arm molecular weights that differ by a factor of 1.3, ω_c is found to increase by a factor of 8. An even more dramatic effect is seen for P1207 and P1210 where a factor of 1.6 difference in arm molecular weight yields close to a 17-fold change in ω_c. These trends are not surprisingly mirrored by the zero shear viscosity η_0 and the polymer disengagement time λ_d (Table 2), indicating that the extra friction $\zeta_a \approx (kT/N_a b^2)\lambda_a$ generated by each arm on the cross-bar, is likely responsible for the dramatic differences seen in all three rheological variables.

Table 2. Rheological Parameters for Linear and Branched Polybutadienes

sample	ω_c^{-1} (s)	λ_k (s)	λ_d (s)	η_0 (Pa·s)	G_N (Pa)
PBD86	0.04		0.04	1.8×10^4	7.6×10^5
PBD129	0.13		0.20	7.4×10^4	7.8×10^5
PBD176	0.33		0.46	2.0×10^5	8.6×10^5
P1134	4.07	18.2	30.26	3.6×10^5	9.8×10^4
P1184	10.86	35.0	66.5	5.8×10^5	4.3×10^4
P1132	32.4	90.8	163.7	1.2×10^6	4.5×10^4
P1210	22.14	210.5	322.3	3.9×10^6	2.5×10^5
P1207	376.5	830.7	1259.1	2.9×10^7	1.0×10^5

Second, over the range of frequencies explored, the storage and loss moduli of the multiarm materials display self-similar frequency dependencies that are distinctly different from typical behavior observed in linear polybutadiene. For instance, at high frequencies the loss moduli for P1184, P1132, and P1134 superpose onto each other and take values somewhat lower than those of PBD129. Similar behavior is seen in Figure 3c,d, where storage and loss moduli of P1207 and P1210 are compared with those of PBD176 and PBD86. In fact, if Figure 3a,c and Figure 3b,d are compared, the storage and loss moduli for all the multiarm polymers appear to collapse on the same curves at frequencies well below where glassy behavior is anticipated, suggesting that arm relaxation dominates dynamics at these frequencies.

Third, storage and loss moduli of the multiarm polybutadienes appear to manifest premature transitions to terminal behavior at shear frequencies well above those where such behavior is ultimately seen. In all cases, the high-frequency terminal transition is arrested at frequencies about two decades higher than ω_c, yielding only kinks or inflection points in the loss and storage moduli. A reasonable estimate for the arm disengagement time is $\lambda_a = \lambda(N_c/N)^{1.5} \exp[15N/8N_e]$.[2] Here $\lambda = \tau_1(N^{3.5}/N_c^{1.5})$ is the tube disengagement time of a linear entangled polybutadiene with the same molar mass as the arm, $N_c \approx 2N_e$ and τ_1 is a monomeric jump relaxation time. Using PBD176 as a reference, the characteristic arm disengagement times for the multiarm polymers used in this study fall in the range $0.35 \le \lambda_a \le 750.0$ s. These times are somewhat longer than theoretical estimates including dynamic dilution $0.008 \le \lambda_a \le 1.13$ s; the separation between arm and cross-bar relaxations evident from the dynamic moduli suggests the arm disengagement time including dynamic

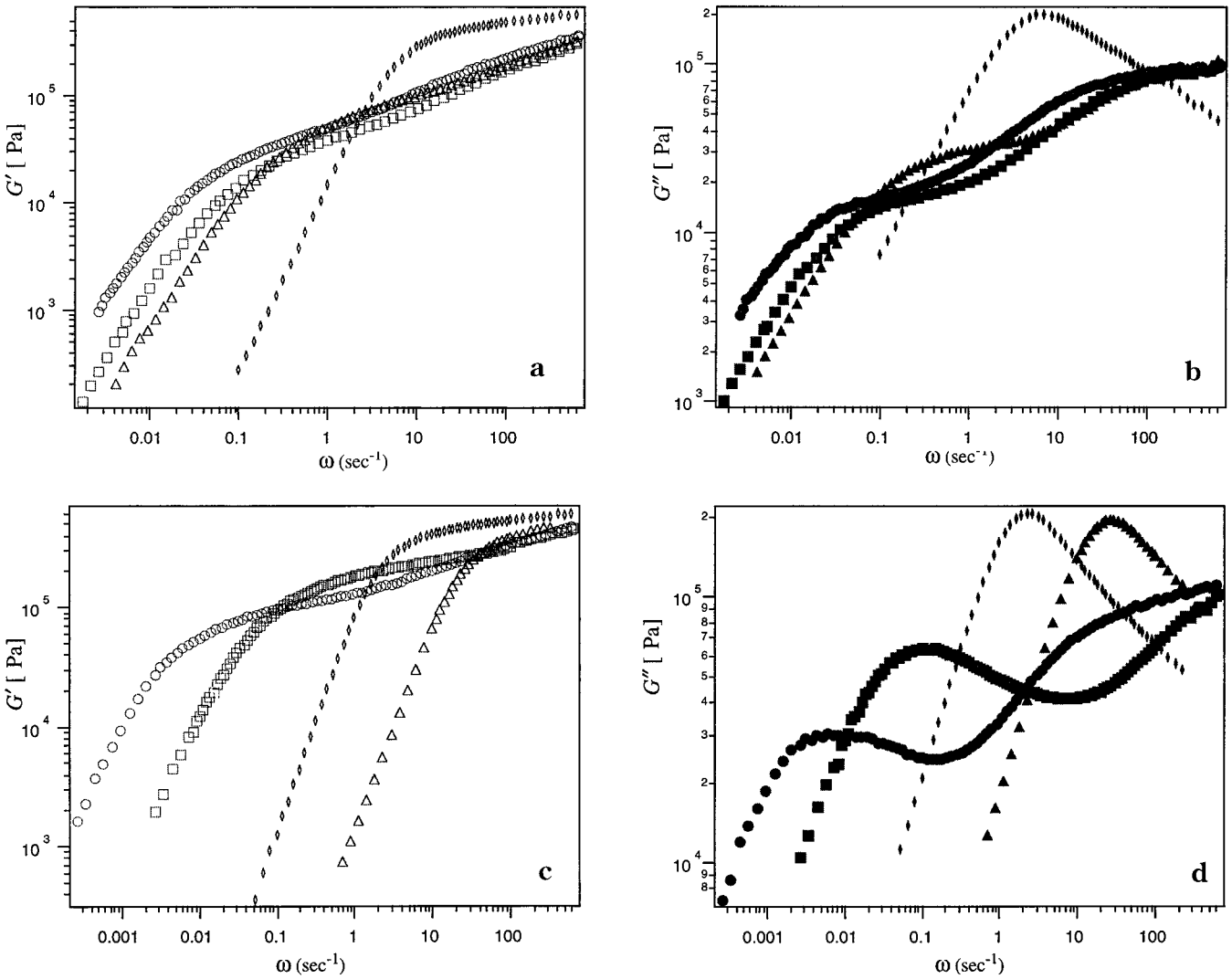

Figure 3. (a) Dynamic storage moduli $G'(\omega)$ for PBD129 (open diamond), P1134 (open triangle), P1184 (open square), and P1132 (open circle) at various shear frequencies, ω. All experiments were performed at 24.5 °C. (b) Dynamic loss moduli $G''(\omega)$ for PBD129 (filled diamond), P1134 (filled triangle), P1184 (filled square), and P1132 (filled circle) at various shear frequencies, ω. All experiments were performed at 24.5 °C. (c) Dynamic storage moduli $G'(\omega)$ for PBD86 (open triangle), PBD176 (open diamond), P1210 (open square), and P1207 (open circle) at various shear frequencies, ω. All experiments were performed at 24.5 °C. (d) Dynamic loss moduli $G''(\omega)$ for PBD86 (filled triangle), PBD176 (filled diamond), P1210 (filled square), and P1207 (filled circle) at various shear frequencies, ω. All experiments were performed at 24.5 °C.

dilution is $\lambda_a = \lambda(N_c/N)^{1.5} \exp[(15N/4N_e)(0.5 - (1 - \phi_B)/3)]$.[13,17] It is apparent that arm disengagement times estimated by the latter method are substantially shorter than the multiarm polymer disengagement times λ_d (Table 2) but are of the correct order of magnitude to account for the premature transition to terminal behavior seen in the multiarm materials.

Large differences in λ_a and λ_d support a clear separation between arm and cross-bar relaxation dynamics, as suggested by the theory.[11,13] However, the effect of arm entanglement density on the actual separation $\Lambda = \lambda_d/\lambda_a$ of the two time scales appear more complex than the theory suggests. For example, the cross-bar entanglement densities of P1210 and P1207 are the same, the theoretical separation ratios should therefore satisfy $(\Lambda_{P1207}/\Lambda_{P1210})_T = (\phi_{b,\,P1207}/\phi_{b,\,P1210}) = 0.75$. Using the experimental λ_d data and the λ_a estimates from above, the actual ratio is found to be substantially smaller: $\Lambda_{P1207}/\Lambda_{P1210}) = 0.065$ (including dynamic dilution) and $(\Lambda_{P1207}/\Lambda_{P1210}) = 0.0018$ (neglecting dynamic dilution). The corresponding theoretical result for P1132 and P1134 is $(\Lambda_{P1132}/\Lambda_{P1134})_T = 0.84$, compared to the experimental values $(\Lambda_{P1132}/\Lambda_{P1134})_T = 0.58$ (including dynamic dilution) and $(\Lambda_{P1132}/\Lambda_{P1134})_T = 0.047$ (neglecting dynamic dilution). Again suggesting a stronger dependence on arm molecular weight than captured by the theory.

Samples P1207 and P1132 have the same arm molecular weights but different cross-bar molecular weights. Their Λ values are $(\Lambda_{P1132}/\Lambda_{P1207})_T = (\Lambda_{d,\,P1132}/\Lambda_{d,\,P1207}) = 0.18$. The experimental ratio of polymer disengagement times (Table 2) is $(\lambda_{d,\,P1132}/\lambda_{d,\,P1207}) = 0.13$, which is in reasonably good agreement with the theoretical result. The better agreement between theory and experiment concerning the effect of cross-bar molecular weight on multiarm polymer relaxation is promising. More work on a wider range of cross-bar molecular weights, for fixed arm molecular weight, is obviously needed before firm conclusions can be reached.

A clear separation of arm and cross-bar relaxation time scales implies that in step strain measurements employing multiarm polymers the measured stress is mostly due to cross-bar orientation and stretch. As seen earlier, however, the dynamic friction constraint due to

the arms remain even after they have relaxed, yielding cross-bar disengagement and stretch relaxation times that are significantly higher than expected for linear polybutadienes of comparable molecular weights. Transient nonlinear step strain relaxation data $G(t;\gamma) \equiv \sigma(t;\gamma)/\gamma$ for P1132 are presented in Figure 4a for shear strains varying from 0.1 to 18.0. For clarity, only a small subset of the results are identified in the legend. These data sets are singled out because, over the range of shear strains covered, a significant and heretofore unreported drop is seen in $G(t;\gamma)$. Remarkably, the drop begins at a shear strain of close to 6.0 ($\langle|E\cdot u|\rangle = 3.2$), which is in near quantitative agreement with the theoretical prediction $\langle|E\cdot u|\rangle = 3.0$ for multiarm polymers with the architecture depicted in Figure 1.[9,10] Curiously, despite the catastrophic microscopic event that is predicted to cause the drop in $G(t;\gamma)$, very little change in the shape of the nonlinear modulus is evident from the data. In fact in Figure 4b,c the relaxation modulus is seen to be separable into time and strain dependent parts $G(t;\gamma) = G_e h(\gamma)\, G(t)$ beyond a characteristic time $\lambda_k \approx 91$ s that shows no obvious change at strains above and below the critical strain for arm withdrawal. This finding appears inconsistent with the theoretical prediction that at shear strains above the critical value, stretch relaxation is replaced by a new branch point withdrawal process with a "characteristic" time scale that is itself time-dependent.[11,13] The original stretch relaxation mechanism observed at strains below the critical shear strain is suspended until after branch point withdrawal is complete.

Similar behavior is observed for all the multiarm polybutadienes, except the value of λ_k varies from polymer to polymer (Table 2). The experimental λ_d/λ_k show little, if any, dependence on cross-bar entanglement density, however, and a simple proportional relationship between λ_k and λ_d can be seen for all the multiarm polymers $\lambda_d = (1.7 \pm 0.2)\lambda_k$ (see Table 3). This observation is quite different from behavior reported for entangled solutions of linear flexible polymers where the separability time appears more closely aligned with a longest Rouse relaxation time than with the chain disengagement or reptation time.[18−20] In linear polymers with modest entanglement densities the separability time is found by both experiment[18] and theory[21] to be 4−5 times larger than the characteristic time scale for stretch relaxation. As shown recently by Archer and Mhetar,[21] the factor of 4−5 results from the fact that the primitive chain contour length requires a period of 4−5 times the characteristic stretch relaxation time to relax to within a percent of its equilibrium value following a nonlinear step strain. At shear strains below the critical value, stretch relaxation in multiarm polymers is thought to occur by a Rouse-like diffusive process with characteristic time scale $\lambda_s = i s_b \lambda_a$ well below the polymer disengagement time $\lambda_d/\lambda_s = (4/\pi^2) s_b \phi_b$ for well-entangled polymers. The experimental $(\lambda_d/\lambda_k)_E$ ratio for each of the polymers studied are compared with theoretical estimates, $(\lambda_d/\lambda_s)_T$, in Table 3. The experimental and theoretical values are seen to be of the same order of magnitude. However, the theoretical values show a dependence on cross-bar molecular weight that is not captured by the experiments.

The "damping" function $h(\gamma)$ required to superpose data taken at different shear strains is presented in Figure 5. This figure also includes $h(\gamma)$ results from

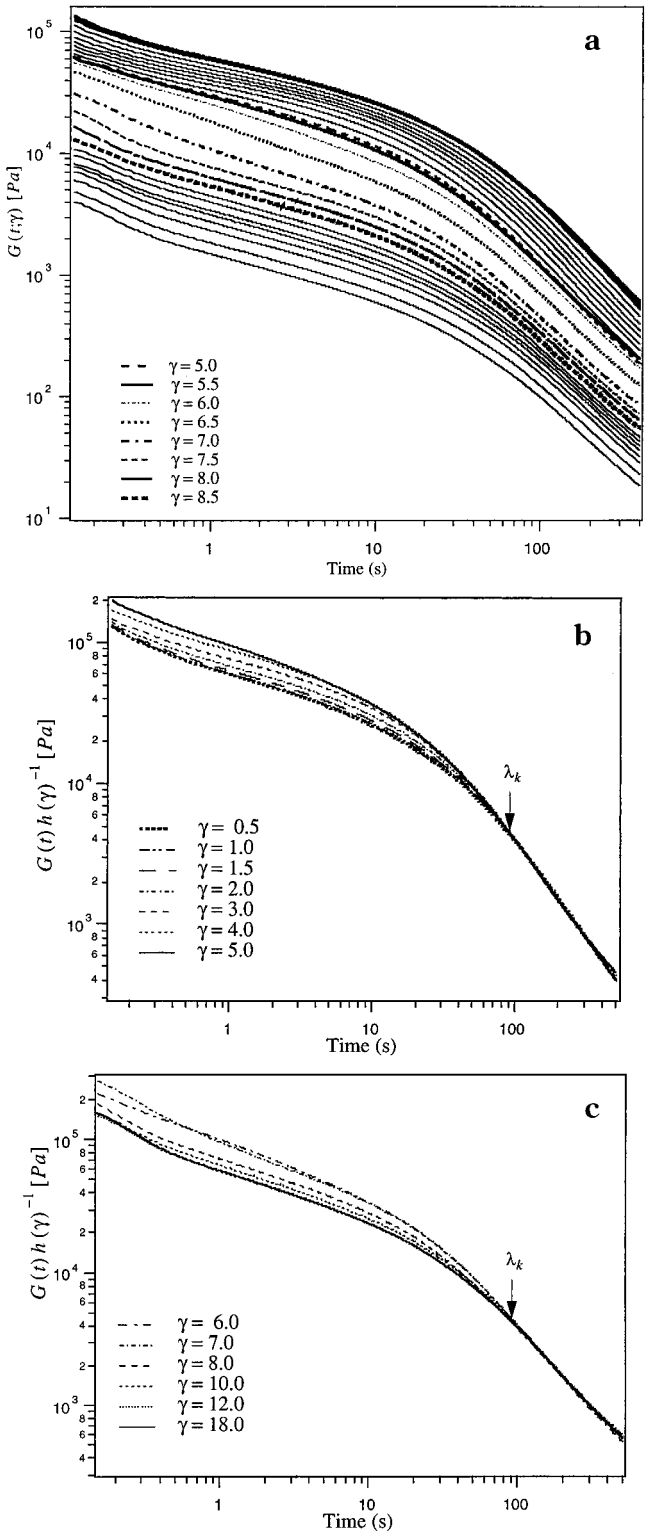

Figure 4. (a) Time-dependent nonlinear relaxation modulus $G(t;\gamma) \equiv (\sigma(t;\gamma))/\gamma$ following step shear strains from 0.1 to 18.0. The time required to impose the desired strain ranged from 0.05 s at low strains to 0.2 s at the highest strain studied. Strain increases from top to bottom in this figure. (b) Time-dependent nonlinear relaxation modulus $G(t;\gamma)h(\gamma)^{-1}$ for shear strains below the critical value $\gamma \approx 6$, ($\langle|E\cdot u|\rangle = 3.2$). The individual $G(t;\gamma)h(\gamma)^{-1}$ curves are obtained by vertically shifting the $G(t;\gamma)$ curves from Figures 4a, each by an amount $-\log h(\gamma)$, so that they superimpose with the lowest-strain curve ($\gamma = 0.1$, in this case) at long times. The *separability time* λ_k is defined as the time beyond which the curves all appear to collapse onto a single line. (c) Same as (b) except for strains slightly below and above the critical value.

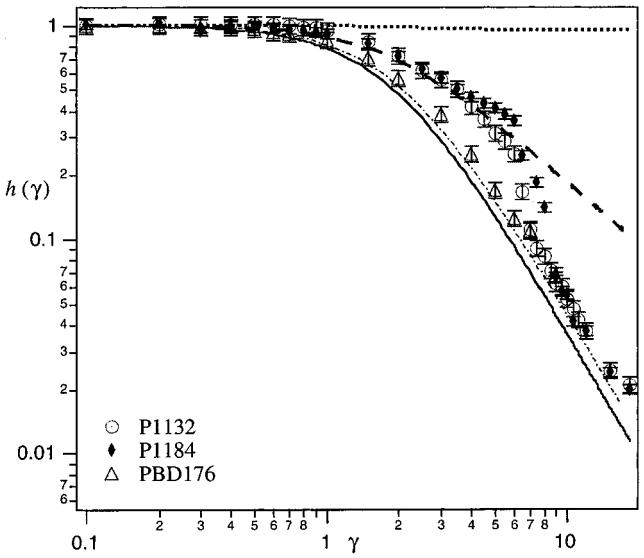

Figure 5. Damping function $h(\gamma)$ for a linear polybutadiene (PBD176) and two of the multiarm materials (P1184 and P1132). The experimental results are compared with the low-strain $h_{el}(\gamma)$ (···) and high-strain $h_{DE}(\gamma)$ (—) damping function predictions of Bick and McLeish.[10] Damping functions determined from the Doi−Edwards theory including the independent alignment assumption,[12] $h_{DEIA}(\gamma)$ (−·−) and from the partial strand extension theory of Mhetar and Archer,[22] $h_{PSE}(\gamma)$ (---) are included for comparison.

Table 3. Comparison of Theoretical and Experimental Stretch Relaxation and Disengagement Times

sample	$(\lambda_d/\lambda_k)_E$	$(\lambda_d/\lambda_s)_T$
P1134	1.66	3.2
P1184	1.90	2.0
P1132	1.80	2.6
P1210	1.53	10.3
P1207	1.52	7.7

P1184 and PBD176 as well as theoretical predictions from the Doi−Edwards $h_{DE}(\gamma)$, Doi−Edwards independent alignment $h_{DEIA}(\gamma)$,[12] partial strand extension $h_{PSE}(\gamma) = 1/(15/4)\gamma\langle(\mathbf{E}\cdot u)(E\cdot u)/|E\cdot u|\rangle$,[22,23] and affine extension $h_{el}(\gamma)$ models. It is apparent from Figure 5 that the damping function for PBD176 is in closer accord with the Doi−Edwards independent-alignment prediction than with the full Doi−Edwards model result. Similar behavior has been reported previously for entangled polystyrene solutions.[18] At low shear strains the data for the multiarm polymers are seen to deviate significantly from the affine extension result computed by assuming that the arms prevent retraction of the cross-bar. In fact, much better agreement is seen with the predictions provided by the partial strand extension model.[22] The reason for this agreement is unclear however. In the partial strand extension model it is contended that, following nonlinear step strains, entangled linear polymers retract to preserve their equilibrium Gaussian structures in a deformed tube. Specifically, Mhetar and Archer show that a step strain of local amplitude $\langle|E\cdot u|\rangle$ induces simultaneous affine extension of a polymer's contour length $L/L_0 = \langle|E\cdot u|\rangle$, and compression of the tube diameter $a/a_0 = \langle|E\cdot u|\rangle^{0.5}$. The deformed polymer can therefore regain its equilibrium Gaussian structure in the new tube environment by retracting to a contour length $L_0\langle|E\cdot u|\rangle^{0.5}$, which could be substantially larger than the equilibrium contour length L_0.[22] That the PSE prediction is in better agreement with the multiarm polymer data than the affine extension result suggests that dynamical processes other than retraction may be available to the cross-bar to facilitate return to a Gaussian chain structure in the deformed tube. More work is clearly needed to establish whether extra relaxation processes, for example, lost cross-bar constraints when arms relax, could help explain the experimental observations.

At shear strains exceeding 6.0 ($\langle|E\cdot u|\rangle = 3.2$) the damping function of the multiarm polymers drop suddenly and approach the Doi−Edwards independent alignment result at shear strains beyond 8.5. This finding is in near perfect agreement with the new proposal for branched polymer dynamics described in the Introduction,[9−11] and provides rather powerful circumstantial evidence for the existence of a mean-field tube. A similar drop in damping function has been reported at lower strains by Kimura et al.[21] for branched polybutadienes with several branches per molecule. In one of the multiarm polymers P1207 the strain at which the damping function decrease is first seen varies from 3.0 to 5, depending on temperature. The lower inception strains are accompanied by ultimate high-strain damping functions below the Doi−Edwards prediction, but showing the same strain dependence as the Doi−Edwards result. More work on other polymers in the P12*xx* series is underway to determine the origin of this behavior.

4.0. Conclusions

We describe the synthesis, linear rheological properties, and nonlinear relaxation dynamics of some novel multiarm polybutadiene molecules in oscillatory shear and step strain experiments. The general architecture of the new polymers is shown in Figure 1. In oscillatory shear the multiarm polymers show much broader relaxation spectra than linear polybutadienes of comparable molecular weight. The source of this spectral broadening appears to be dramatic slowing down of cross-bar dynamics by the entangled arms. In nonlinear step strain experiments the arms have an even more remarkable effect on polymer dynamics. At a critical shear strain of around 6.0 ($\langle|E\cdot u|\rangle = 3.2$) a clear drop is seen in the nonlinear relaxation modulus $G(t;\gamma)$. This drop is reflected in the damping function and appears a consequence of arm withdrawal into the tube confining the cross-bar. This behavior is in excellent agreement with predictions of a recent theory by McLeish et al.[9−11,13]

Acknowledgment. We are grateful to the National Science Foundation (Grant No. CMS-9713372) and to the Texas Higher Education Coordinating board for supporting this work.

References and Notes

(1) Graessley, W. W. *Acc. Chem. Res.* **1977**, *10*, 332.
(2) Pearson, D. S.; Helfand, E. *Macromolecules* **1984**, *17*, 888.
(3) Roovers, J. *J. Non-Cryst. Solids* **1991**, *131*, 793.
(4) Adams, C. H.; Hutchings, L. R.; Klein, P. G.; McLeish, T. C. B.; Richards, R. W. *Macromolecules* **1996**, *29*, 5717.
(5) Roovers, J.; Graessley, W. W. *Macromolecules* **1981**, *14*, 766.
(6) Yurasova, T. A.; McLeish, T. C. B.; Semenov, A. N. *Macromolecules* **1994**, *27*, 7205.
(7) Roovers, J.; Toporowski, P. *Macromolecules* **1981**, *14*, 1174.
(8) Roovers, J. *Macromolecules* **1984**, *17*, 1196.
(9) McLeish, T. C. B. *Macromolecules* **1988**, *21*, 1062.
(10) Bick, D. K.; McLeish, T. C. B. *Phys. Rev. Lett.* **1996**, *76*, 2587.
(11) Bishko, G.; McLeish, T. C. B.; Harlen, O. G.; Larson, R. G. *Phys. Rev. Lett.* **1997**, *79*, 2352.

(12) Doi, M.; Edwards, S. F. The Theory of Polymer Dynamics; Oxford University Press: Oxford, U.K., 1986.
(13) McLeish, T. C. B.; Larson, R. G. *J. Rheol.* **1998**, *42*, 81.
(14) Ferry, J. D. Viscoelastic Properties of Polymers, 2nd ed.; John Wiley: New York, 1970.
(15) Yu. Y. S.; Dubois, Ph.; Jerome, R.; Teyssie, Ph. *Macromolecules* **1996**, *29*, 2738.
(16) Hakki, A.; Young, R.; McLeish, T. C. B. *Macromolecules* **1996**, *29*, 3639.
(17) McLeish, T. C. B.; O'Connor, K. P. *Polymer* **1993**, *34*, 2998.
(18) Osaki, K.; Nishizawa, K.; Kurata, M. *Macromolecules* **1982**, *15*, 1068.
(19) Ball, R. C.; McLeish, T. C. B. *Macromolecules* **1989**, *22*, 1911.
(20) Osaki, K. *Rheol. Acta* **1993**, *32*, 429.
(21) Archer, L. A.; Mhetar, V. R. *Rheol. Acta* **1998**, *37*, 170.
(22) Mhetar, V. R.; Archer, L. A. *J. Non-Newtonian Fluid Mech.*, in press.
(23) Kimura, S.; Osaki, K.; Kurata, M. *J. Polym. Sci., Polym. Phys. Ed.* **1981**, *19*, 151.

MA9802733